Diabetes mellitus and the metabolic syndrome do not abolish, but might reduce, the cardioprotective effect of ischemic postconditioning

Wouter Oosterlinck, MD,[a] Tom Dresselaers, PhD,[b] Vincent Geldhof,[a] Ines Nevelsteen, MD,[a] Stefan Janssens, MD, PhD,[c] Uwe Himmelreich, PhD,[b] and Paul Herijgers, MD, PhD[a]

Objective: Ischemic preconditioning fails to protect the diabetic heart against lethal reperfusion injury. Because the pathways of ischemic pre- and postconditioning partially overlap, we evaluated the cardioprotective effect of ischemic postconditioning in mouse models of type 2 diabetes (ObOb) and the metabolic syndrome (DKO).

Methods: Mice (C57BL/6J, ObOb, and DKO; aged 24 weeks; n = 24, n = 28, and n = 18, respectively) underwent reperfusion after 30 minutes of coronary occlusion with or without ischemic postconditioning (3 cycles of 10 seconds reperfusion–reocclusion). Left ventricular contractility and infarct size were assessed 60 minutes later with pressure conductance analysis and 2,3,5-triphenyl-tetrazolium chloride staining, respectively. In a second cohort (C57BL/6J and DKO; aged 12 weeks; n = 31 and n = 24, respectively) cardiac cine magnetic resonance imaging was performed after 1 and 10 weeks, followed by pressure conductance analysis and Sirius red staining.

Results: In the C57BL6/J mice, the infarct size was lower (40%, $P < 10^{-5}$) and the load independent preload recruitable stroke work was greater after ischemic postconditioning ($P < .05$). In the ObOb and DKO mice, ischemic postconditioning reduced the infarct size by 24% ($P < 10^{-5}$). In the C57BL/6J mice, the ejection fraction was greater and the myocardial mass was lower 10 weeks after ischemic postconditioning ($P < .05$). Tagging grid deformation was increased after ischemic postconditioning in both infarcted and remote areas. After ischemic postconditioning, the survival and ejection fraction were greater in the DKO mice (67% vs 17% and 44% ± 11% vs 59% ± 2%, $P < .05$ for both), and the collagen content was lower for both C57BL/6J and DKO mice ($P < .05$ for both).

Conclusions: The cardioprotective effect of ischemic postconditioning was sustained in C57BL/6J mice after 10 weeks and protected against adverse left ventricular remodeling. In mouse models of type 2 diabetes, protection against lethal reperfusion injury is present, leading to increased survival after ischemia and reperfusion. (J Thorac Cardiovasc Surg 2013;145:1595-602)

Ischemic postconditioning (IPostC) protects the heart against lethal reperfusion injury. The protective effect of intermittent ischemic events at the beginning of the reperfusion period was first described by Zhao and colleagues[1] in 2003 and demonstrated the relevance of lethal reperfusion injury. A series of repetitive cycles of brief reperfusion and reocclusion of the coronary artery applied at the onset of reperfusion after a prolonged ischemic event reduced the infarct size in a canine model. This finding has been confirmed in numerous investigations performed in mice,[2] rats,[3,4] rabbits,[5,6] pigs,[7] and humans[8-10]; however, data on the long-term benefit remains scarce.[11]

A paucity of experimental investigations has been done to determine the effect of comorbidities such as hyperlipidemia, diabetes, or obesity on IPostC, because most studies investigating postconditioning have been conducted using healthy animals. Obesity and diabetes mellitus are not only major risk factors for myocardial infarction, but also impair the prognosis in cardiovascular diseases[12] and during cardiac surgery.[13] Patients with these risk factors represent a considerable proportion of patients presenting to the cardiac surgical department. Several pathways have proved essential in the mechanism of IPostC protection,[14-17] and confounders interacting with these mechanisms have been suggested.[18] Because preconditioning fails to protect the heart in patients with diabetes mellitus type 2,[19] and the preconditioning and postconditioning pathway partially overlap, the clinical relevance of these confounding factors is not a futile question.

Therefore, we investigated the infarct size–limiting and functional effects of IPostC in a mouse model of type 2

PM

diabetes (ObOb: leptin deficiency causing obesity and type 2 diabetes mellitus) and a mouse model of the metabolic syndrome (ob/ob and low-density lipoprotein receptor$^{-/-}$ knockout: DKO with type 2 diabetes mellitus, obesity, dyslipidemia, and atherosclerosis) using left ventricular (LV) pressure conductance (PC) analysis and infarct size determination. We also studied long-term cardiac postischemic remodeling using cine magnetic resonance imaging (cMRI) with myocardial tagging and LV PC analysis after 10 weeks.

METHODS
Animal Models and Surgical Procedures
The mice were housed at 22°C on a fixed 12-hour light/dark cycle. The investigation conformed to the ''Guide for the Care and Use of Laboratory Animals'' (National Institutes of Health, NIH publication no. 85-23, revised 1996, Bethesda, Md). The institutional animal care commission and ethical committee of the KU Leuven approved all experimental protocols.

We studied a mouse model of type 2 diabetes (ObOb: leptin deficiency causing obesity and type 2 diabetes) and a mouse model of the metabolic syndrome (ob/ob and low-density lipoprotein receptor$^{-/-}$ knock-out: DKO showing type 2 diabetes, obesity, dyslipidemia, and atherosclerosis). All mice were fed standard chow, containing 4% fat (Pavan Service, Oud-Turnhout, Belgium). The mice had been backcrossed for at least 10 generations into the C57BL/6J background, and all mice had a 98.4% C57BL/6J background. Homozygous Ob/Ob mice were purchased from Jackson Laboratory (Bar Harbor, Maine). Homozygous DKO mice were generated as previously described.[20]

Ischemia–Reperfusion Experiments
Short-term study. One week before the surgical procedure, an intraperitoneal glucose tolerance test was performed with a bolus glucose injection of 2 mg/g body weight after 12 hours of fasting. The blood glucose levels were measured before injection and 15, 30, 60, 120, and 240 minutes after by tail blood withdrawal.

At 24 weeks, the mice (C57BL/6J, n = 24; Ob/Ob, n = 28, and DKO, n = 18) were anesthetized with a mixture of urethane (1.2 g/kg) and alfa-chloralose (50 mg/kg) intraperitoneally. The rectal temperature was kept at 36.0°C to 37.5°C. A tracheostomy was performed, and mechanical ventilation (Minivent 845; Hugo Sachs/Harvard Apparatus, March-Hugstetten, Germany) was started with 50% oxygenated air, tidal volume

of 3 × body weight + 155 μL, and respiratory rate of 135 strokes/min. A thoracotomy through the left fourth intercostal space was performed. Occlusion of the left anterior descending artery was performed by a tourniquet with a pulley system to allow reproducible occlusion with a standardized weight (6 g). The cycle was 30 minutes of ischemia followed by 60 minutes of reperfusion. In the IPostC group, the first minute of reperfusion was interrupted by 3 × 10 seconds of reocclusion/reperfusion. In the sham operated mice (n = 6, C57BL/6J; n = 6, DKO; n = 8, ObOb), a thoracotomy was performed without occlusion of the left anterior descending artery. Finally, the functional evaluation was performed using PC analysis and infarct size determination after administration of Evans blue stain, followed by cardiac arrest within 30 seconds and excision of the heart.

Long-term study. In the long-term study experiments, C57BL/6J (healthy wild-type [WT]) and DKO mice (both aged 12 weeks, C57BL/6J, n = 31; DKO, n = 24) were anesthetized with pentobarbital (50 mg/kg), xylazine (2 mg/kg), ketamine (30 mg/kg), and atropine (0.03 mg/kg) to allow transoral endotracheal intubation and achieve surgical anesthesia. The surgical procedure was performed as described for the short-term study. The blood glucose levels were measured for 1 day. After closure of the chest, the mice were weaned from the ventilator and extubated.

cMRI with myocardial tagging at 1 and 10 weeks after surgery was followed by PC analysis. Finally, the mice were killed by excision of the heart. The hearts were weighed, and the tibial length (TL) was determined.

Functional Evaluation
PC analysis. PC analysis was performed with a 1.4F, high-fidelity pressure-conductance catheter (SPR-839; Millar Instruments, Houston, Tex) inserted through the right carotid artery into the left ventricle. The LV pressure-conductance measurements were started after 45 minutes of reperfusion in the short-term study and after 10 weeks in the long-term study. After stabilization of the hemodynamic situation, baseline pressure–volume (PV) loops were recorded (Powerlab/4SP ADInstruments, Castle Hill, Australia). The inferior caval vein was compressed with a cotton swab without opening the abdomen, and the PV loops were recorded to obtain occlusion loops with a progressively lowering preload. A parallel volume was determined by a bolus injection of 3 μL of 30% sodium chloride solution in the left jugular vein, while recording the PV loops. Afterward, 300 μL of blood was retrieved from the inferior caval vein to measure the specific conductivity in 3 precalibrated cuvets. After calibration, the load-dependent and load-independent contractility parameters were calculated. The load-independent measurements included the end-systolic elastance (Ees), V0 intercept, preload recruitable stroke work (PRSW), end-diastolic pressure–volume relationship, and relaxation coefficient tau.

Micro-magnetic resonance imaging. cMRI was performed after 1 and 10 weeks using a Bruker Biospec, 9.4 Tesla, small animal MRI scanner (Bruker BioSpin, Ettlingen, Germany; horizontal bore, 20 cm) equipped with an actively shielded gradient insert (1200 mT/m) and a 3.5-cm quadrature coil (Bruker Biospin). For localization purposes, 2-dimensional electrocardiographically triggered pseudo short-axis and long-axis T$_1$-weighted images were recorded (fast low angle shot, excitation time, 1.5 ms; repetition time, 5 ms; flip angle, 17°; matrix 256 × 256, field of view, 30 × 30 mm; slice thickness, 500 μm). A stack of short-axis images was then recorded from the base to the apex (at end-systole; 15-20 frames, depending on the heart rate) followed by mid-level and apical tagging imaging (spatial modulation of magnetization preparation and 2-dimensional fast low angle shot cine sequence with specific parameters: repetition time, 9.9 ms; excitation time, 2.5 ms; flip angle, 20°; tag spacing, 400 μm, tag thickness, 100 μm; field of view, 30 × 30 mm; 0.6-ms block pulse of 20°, 15 averages using both electrocardiographic and respiration triggering, 15 frames to cover the entire cardiac cycle over 2 QRS complexes). The volumes and ejection fraction (EF) were calculated using purpose-developed analytic software.[21] The papillary
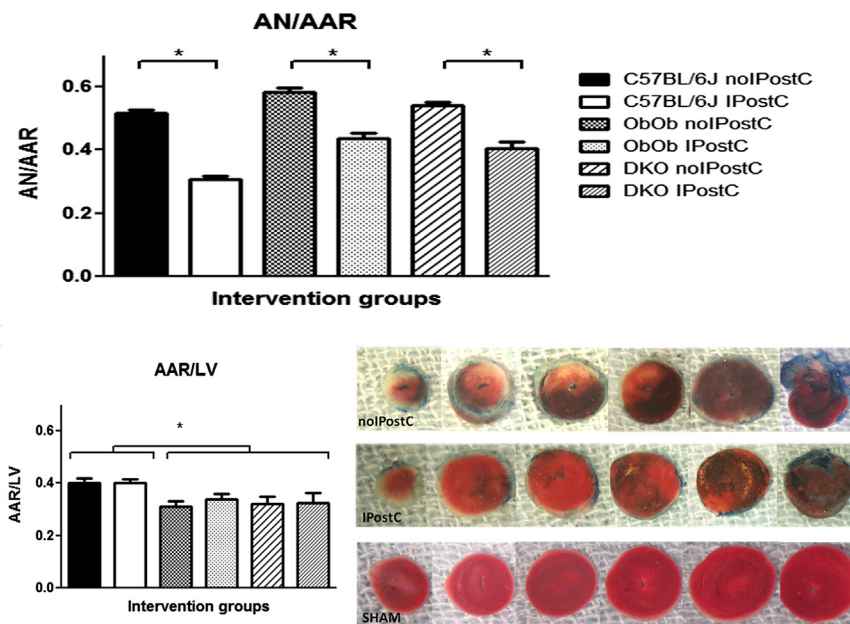
FIGURE 1. Area of necrosis/area at risk *(AN/AAR),* AAR/left ventricular *(LV),* and representative histologic slices from the no ischemic postconditioning *(noIPostC),* ischemic postconditioning *(IPostC),* and sham groups in the short-term study. The AN/AAR was 40% smaller after IPostC than after no IPostC. In both ObOb and DKO mice, IPostC reduced the AN/AAR by 24%. The interaction between IPostC and the study group (healthy, ObOb, DKO) on infarct size reduction did not reach statistical significance. *P < .05.

muscles were considered part of the ventricular volume. Tagging grid deformation analysis was performed using Diagnosoft VIRTUE, version 4.0, software (Diagnosoft, Morrisville, NC).

Deformation imaging of the LV midwall circumferential shortening (circumferential strain) can be determined using the Lagrangian or Eulerian strain. The Lagrangian strain is defined as the change in length divided by the original length, and the Eulerian strain is the strain divided by the instantaneous length. We chose to report the Eulerian strain data because of the high heart rate in rodents and the relatively limited frame rate in myocardial tagging; thus, this relative approach theoretically allowed a more independent determination of strain and deformation.

Histologic Examination
Short-term study. Evans blue stain (0.8 mL, 1% solution) was injected in the left jugular vein during left anterior descending artery reocclusion to determine the LV perfusion area at risk (AAR). The heart was excised and placed in tissue freezing medium (Tissue-Tek, Sakura Finetek, Torrance, Calif) in a -20°C freezer for at least 1 hour. With a custom-made razorblade system, the heart was cut in slices of 1 mm thickness. These slices were placed for 20 minutes in 2,3,5-triphenyl-tetrazolium chloride solution (1%, 37°C, phosphate buffer, pH 7.4). Next, the slices were placed for 10 minutes in paraformaldehyde (4% solution, 20°C). All slices were weighed and photographed with a digital camera under microscopic magnification, and pixel analysis was performed with Adobe Photoshop, CS5 (Adobe Systems, San Jose, Calif). The infarct size was normalized for the AAR, resulting in the area of necrosis over the AAR.

Long-term survival group. The myocardial tissue was rinsed after excision of the heart with sodium chloride 0.9%, fixed overnight in Z-fix 20% (catalog no. 171; Anatech, Battle Creek, Mich) and embedded in paraffin. Sirius red staining for collagen was performed on 3-μm-thick slices at the basal, mid, and apical slices, followed by planimetry with Zeiss Axiovision, version 4.8, software (Carl Zeiss Canada, Toronto, Ontario, Canada), to calculate an indexed collagen content over the area of left ventricle.

Statistical Analysis
Statistical analysis was performed with GraphPad Prism, version 5.04 (GraphPad Software, La Jolla, Calif) and Statistica, version 8.0 (StatSoft, Tulsa, Okla). All data are expressed as the mean $\pm$ standard error. The mean differences between groups were analyzed using 1-way analysis of variance, with Bonferroni post hoc testing. A factorial analysis of variance, shams excluded, was performed to determine the interaction between IPostC and study group (healthy, ObOb, DKO) on infarct size reduction. No significant deviations from normality were observed for model residuals and variances between groups were equal for reported values. P < .05 was used to denote statistical significance.

RESULTS
Short-Term Effect of IPostC in ObOb and DKO Mice Versus Healthy C57BL/6J Mice
The intraperitoneal glucose tolerance test at 23 weeks in ObOb and DKO mice versus C57BL/6J mice showed greater fasting (202 $\pm$ 18 and 203 $\pm$ 16 mg/dL vs 62 $\pm$ 7 mg/dL; P < .001) and peak glycemic (564 $\pm$ 13 and 523 $\pm$ 21 mg/dL vs 455 $\pm$ 22 mg/dL; P < .05) values, and an increased area under the glycemic curve in time (1837 $\pm$ 73 mg/h/dL and 1681 $\pm$ 92 mg/h/dL vs 810 $\pm$ 28 mg/h/dL; P < .001) after a 2-mg/g bolus glucose injection. The body weight was significantly greater in the ObOb and DKO mice than in the C57BL/6J mice at 24 weeks (63 $\pm$ 1 and 60 $\pm$ 2 g vs 27 $\pm$ 1 g, respectively; P < .001).

In the C57BL/6J mice, the area of necrosis/AAR (Figure 1) was 40% smaller after IPostC than after no IPostC. The contractility, reflected by the Ees and PRSW,

PM

TABLE 1. Infarct size, Ees, and PRSW in no IPostC, IPostC, and sham groups in C57BL/6J, ObOb, and DKO mice

| Mode of reperfusion (subjects/group)	AN/AAR	Ees (mm Hg/μL)	PRSW (mm Hg)
C57BL6/J			
No IPostC (n = 12)	0.52 ± 0.01*	7.1 ± 0.6†,‡	46 ± 4†,‡
IPostC (n = 6)	0.31 ± 0.02	11.2 ± 1.2	69 ± 4†,‡
Sham (n = 6)	NA	12.9 ± 1.1	92 ± 11
ObOb			
No IPostC (n = 10)	0.58 ± 0.02*	4.9 ± 0.4†,‡	44 ± 5†,‡
IPostC (n = 10)	0.44 ± 0.02	7.6 ± 0.8	67 ± 7
Sham (n = 8)	NA	7.4 ± 0.9	76 ± 3
DKO			
No IPostC (n = 6)	0.54 ± 0.01*	4.4 ± 0.2†,‡	51 ± 6†
IPostC (n = 6)	0.41 ± 0.02	7.2 ± 0.9	58 ± 5
Sham (n = 6)	NA	8.0 ± 1.1	76 ± 4

Infarct size reduced 40% after IPostC in C57BL/6J mice and 24% in ObOb and DKO mice; Ees significantly greater after IPostC vs no IPostC in all intervention groups; and PRSW significantly greater after IPostC vs no IPostC in C57BL/6J and ObOb mice. *Ees,* End-systolic elastance; *PRSW,* preload recruitable stroke work; *IPostC,* ischemic postconditioning; *AN/AAR,* area of necrosis/area at risk; *NA,* not applicable. *P < .001 vs IPostC. †P < .05 vs sham. ‡P < .05 vs IPostC.

was better after IPostC than after no IPostC (Table 1). In both ObOb and DKO mice, IPostC reduced the area of necrosis/AAR by 24%. The interaction between IPostC and the study group (healthy, ObOb, DKO) on infarct size reduction did not reach statistical significance [$F(2,43) = 2.88$, $P = .067$]. The Ees and PRSW were improved in the ObOb group after IPostC, and the Ees was improved in the DKO group (Table 1).

Long-Term Effect of the Metabolic Syndrome

Survival and glycemic changes during the procedure. The survival in the C57BL/6J mice during the surgical procedure and follow-up period was 100%. In the DKO mice, survival after ischemia–reperfusion was greater after IPostC (67%) than after no IPostC (17%; Figure 2). Most deaths occurred during the first 3 days after the procedure. One mouse died in the no IPostC group after anesthesia induction for the final PC analysis. We measured the glycemic changes intraoperatively to rule out acute hypoglycemia. Greater peak glucose values were registered in the DKO mice (566 ± 13 vs 353 ± 22 mg/dL in the WT mice; P < .001), with normalization after 5 to 7 hours in both DKO and WT mice (312 ± 24 and 165 ± 12 mg/dL; P > .05 vs the preoperative value). The body weight was significantly greater in the DKO mice than in the C57BL/6J mice at 12 weeks (39 ± 2 vs 23 ± 1 g; P < .001).

Functional changes after ischemia–reperfusion. In vivo cMRI (Table 2) showed larger end-systolic and end-diastolic volumes and reduced EF in C57BL/6J at both 1 and 10 weeks in the no IPostC versus IPostC and sham group (both P < .05). The myocardial mass was greater in the no IPostC group than in the IPostC and sham groups
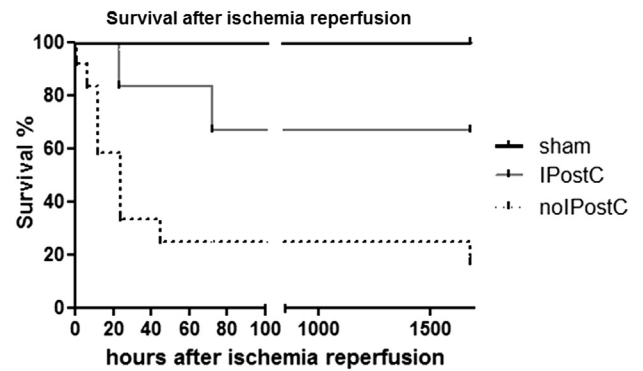
FIGURE 2. Survival curve for DKO mice during 10 weeks of follow-up after ischemia–reperfusion at 12 weeks. In DKO mice, survival after ischemia–reperfusion was greater after IPostC (67%) than after no IPostC (17%). Most deaths occurred during the first 3 days after the procedure. One mouse died after no IPostC after induction for the final pressure conductance analysis.

at 10 weeks (P < .05). In the surviving DKO mice, volumetric changes showed similar trends, with a significant difference in EF induced by IPostC, after both 1 and 10 weeks (vs no IPostC; Table 2) with no difference in myocardial mass measurable.

The in vivo regional contractility analysis, using tagging MRI (Figure 3) was performed by studying the individual Eulerian strain curves, the calculated area under the

TABLE 2. EDV, ESV, LV mass, SV, and EF in C56BL/6J and DKO groups at 1- and 10-week follow-up examinations with cMRI

Group	EDV (μL)	ESV (μL)	LV mass (mg)	SV (μL)	EF (%)
C57BL/6J					
Week 1					
No IPostC	65 ± 4*,†	36 ± 3*,†	67 ± 2	30 ± 3	45 ± 2*,†
IPostC	48 ± 3	19 ± 2	60 ± 3	30 ± 2	60 ± 2
Sham	47 ± 4	17 ± 2	58 ± 3	30 ± 2	65 ± 2
Week 10					
No IPostC	68 ± 4*,†	37 ± 4*,†	72 ± 4*,†	30 ± 2	45 ± 3*,†
IPostC	52 ± 4	24 ± 2	61 ± 2	28 ± 2	55 ± 2
Sham	49 ± 5	20 ± 3	56 ± 3	30 ± 2	61 ± 3
DKO					
Week 1					
No IPostC	53 ± 1	31 ± 1*,†	61 ± 0	22 ± 0	43 ± 9*,†
IPostC	44 ± 0	17 ± 0	56 ± 0	28 ± 0	63 ± 2
Sham	46 ± 0	18 ± 0	58 ± 0	28 ± 0	61 ± 3
Week 10					
No IPostC	52 ± 0	29 ± 1	73 ± 1	23 ± 1*,†	44 ± 11*,†
IPostC	53 ± 0	22 ± 0	65 ± 1	32 ± 0	59 ± 2
Sham	61 ± 0	22 ± 0	56 ± 0	39 ± 0	64 ± 2

EDV and ESV were larger and EF was lower after 1 and 10 weeks of follow-up after no IPostC. Myocardial mass was higher in the no IPostC group than in the IPostC and sham groups at 10 weeks. *EDV,* End-diastolic volume; *ESV,* end-systolic volume; *LV,* left ventricular; *SV,* stroke volume; *EF,* ejection fraction; *cMRI,* cine magnetic resonance imaging; *IPostC,* ischemic postconditioning. *P < .05 vs sham. †P < .05 vs IPostC.
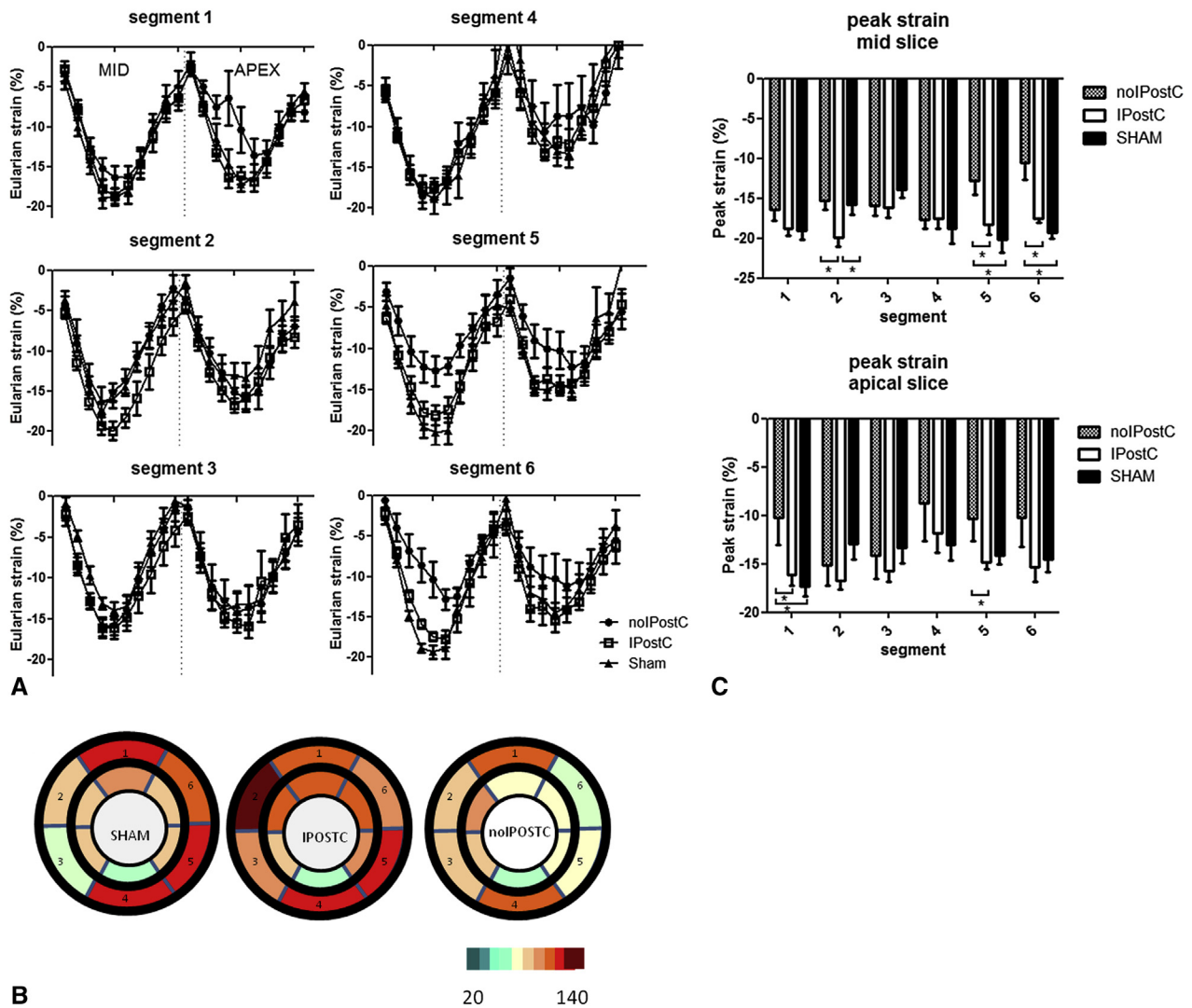
FIGURE 3. Myocardial tagging in C57BL/6J mice after 10 weeks of follow-up for no ischemic postconditioning *(noIPostC),* ischemic postconditioning *(IPostC),* and sham groups. A, Individual circumferential Eulerian strain curves are shown at the mid and apical level of the no IPostC, IPostC, and sham groups. B, Bull's eye plot of the area under the curve (in %*frame) of the Eulerian strain curves at the different segments during the cardiac cycle. Segment 2 represents the interventricular septum in which the supranormal Eulerian strain values were observed after IPostC. C, Peak strain curves of the intervention groups at the 6 segments. Myocardial tagging magnetic resonance imaging *(MRI)* showed less grid deformation after no IPostC in the anterolateral wall (infarcted area, segment 5 and 6). The grid deformation in the anterolateral wall was restored by IPostC, and the interventricular septum (remote area, segment 2) showed significantly more deformation than in the no IPostC and sham groups. *$P < .05$.

glycemic curve, and peak strain values throughout the cardiac cycle. Myocardial tagging MRI showed less grid deformation after no IPostC in the anterolateral wall (infarcted area, segment 5 and 6). The grid deformation in the anterolateral wall was restored by IPostC, and the interventricular septum (remote area, segment 2) showed significantly more deformation than in the no IPostC and sham groups. Consistent with the peak strain analysis, the area under the curve was lower in the infarcted area and greater in segment 2.

No significant differences were present in the Ees, V0, tau, or end-diastolic pressure–volume relationship in the WT mice in the IPostC group versus the no IPostC group.

The PRSW was lower in the no IPostC group (43 ± 4 vs 74 ± 3 mm Hg in the IPostC group and 87 ± 4 mm Hg in the sham group, both $P < .01$) in the C57BL/6J mice. In the DKO mice, the number of mice surviving the experimental procedure and invasive PC analysis was too small to draw conclusions on contractility (n = 1/12 in the no IPostC group, 4/6 in the IPostC group, and 6/6 in the sham group).

Morphologic and histologic data. In the C57BL/6J mice, the heart weight (HW) and HW corrected for the TL were significantly greater in the no IPostC group than in the sham and IPostC groups (126 ± 6 mg and 69 ± 3 mg/μm

vs 105 ± 4 mg and 58 ± 2 mg/μm in the IPostC group and 102 ± 5 mg and 57 ± 3 mg/μm in the sham group, both $P < .01$) confirming our findings from the myocardial mass measurements through cMRI. In the DKO mice, the HW and HW corrected for the TL was not significantly different in the studied groups.

The index of collagen content in the LV wall was greater in the no IPostC group for the C57BL/6J mice (0.10 ± 0.01 vs 0.04 ± 0.01 in the IPostC group and 0.02 ± 0.00 in the sham group, both $P < .01$) and for DKO mice (0.09 ± 0.02 vs 0.03 ± 0.01 in the IPostC group and 0.01 ± 0.00 in the sham group, both $P < .05$).

DISCUSSION

Preclinical studies have suggested that diabetes[22] or the metabolic syndrome[23] increase the threshold for endogenous cardioprotective mechanisms or might even make them impossible.[24] Therefore, it is essential to establish whether a novel cardioprotective strategy is effective in the presence of 1 or more of these comorbidities.

In the present study, we first evaluated the short-term effect of diabetes and the metabolic syndrome on the protective effects of postconditioning. Second, we determined the long-term effects of IPostC using both invasive and noninvasive measurements.

Short-Term Effect of IPostC in ObOb and DKO Mice Versus Healthy C57BL/6J Mice

The results from our short-term experiments confirmed that IPostC reduces the infarct size and LV impairment in C57BL6/J mice, as previously reported.[2] The interaction between IPostC and study group (healthy, ObOb, and DKO) on infarct size reduction did not reach statistical significance, possibly because of the sample size; however, a trend was seen for less infarct size reduction, especially in DKO mice. Nonetheless, IPostC improved the EF and load-independent contractility parameters (Table 1), proving that IPostC is also relevant in subjects with diabetes mellitus and the metabolic syndrome.

Long-Term Effect in Healthy Mice Versus the Metabolic Syndrome

The main function of cardioprotection is, however, to improve function and outcome in the long term, thereby surpassing the observations showing a difference in troponin release. Some investigators have questioned the relevance of the long-term effect of IPostC.[25] The presence of comorbidities might influence the overall effect of an infarct size reduction, in addition to the physical reduction in infarct size alone. Given the trend toward less infarct size reduction in both the ObOb and DKO mice, we wanted to evaluate the effect on remodeling, specifically in the DKO mice, because

they constitute a distinct combination of these hazardous comorbidities.

Survival and glycemic changes during the procedure. We have shown for the first time that, consistent with a smaller infarct size, survival increased after IPostC in an experimental model of the metabolic syndrome. Although survival could potentially be influenced by many factors, the environmental and intraoperative parameters (duration of ischemia, ventilator settings, glycemic changes throughout the procedure) were similar among the experimental groups. Mortality was greatest in the first 72 hours after the ischemia–reperfusion experiment. This underlines the immediate benefit that could be obtained by applying IPostC in a population with diabetes mellitus type 2 and the metabolic syndrome.

Functional changes after ischemia–reperfusion. In our long-term experiments in WT mice, cardiac function improved after IPostC at 1 week, as evidenced by the greater EF and lower end-diastolic volume. However, only after 10 weeks of follow-up was a significant difference in myocardial mass measurable, with increased strain values in the interventricular septum (remote area) and the anterolateral wall (infarcted area) after IPostC. The cardioprotective effect of IPostC was thus sustained after 10 weeks and protected against adverse LV remodeling with a specific contractility pattern revealed by myocardial tagging. The functional changes can be partially explained by the reduced area of infarcted myocardial tissue after IPostC, which we measured using Sirius red staining. However, these also suggest an improved compensation by the remaining remote zone, such as we showed with myocardial tagging, demonstrating even supranormal values after IPostC. We were unable to measure enough mice per group to evaluate differences in invasive PC analysis in the DKO mice. The noninvasive MRI measurements, however, showed a greater EF and stroke volume 10 weeks after IPostC (Table 2). The myocardial mass was not significantly different in the DKO mice. This could have been because only the DKO mice with a smaller infarct size after no IPostC survived or because of a different remodeling process in diabetic mice.

The additional information from our survival experiments was not only the significant improved survival after ischemia, with reperfusion in the diabetic mice, but also the improved regional contractility pattern.

Morphologic and histologic findings. Collagen deposition after 10 weeks was significantly decreased after IPostC in the DKO mice. The reduction was similar to that in the healthy C57BL/6J mice. The HW and the HW corrected for the TL were reduced after IPostC compared with no IPostC in the healthy C57BL/6J mice, in accordance with our noninvasive myocardial mass measurements. However, in the DKO mice, the myocardial mass was not significantly different in the IPostC, no IPostC, or sham group. This

suggests that either a different type of remodeling occurs in these animal models or that a survival bias created lower myocardial mass and intracardiac volumes.

Our findings in light of previous research. The functional benefit of IPostC during percutaneous coronary intervention[8] and beating heart cardiac surgery[26] has been proved by others and has been successfully applied in pediatric cardiac surgery.[27] However, the results from phase II cardioprotection trials have been disappointing to date, probably owing to a lack of knowledge on the protective effects in different disease models and confounding factors.[28]

Bouhidel and colleagues[2] did not find a significant benefit for IPostC in male ObOb mice at 10 weeks after 24 hours of reperfusion, and the infarct size was even larger compared with the size in healthy C57BL/6J mice. However, in our short- and long-term studies, we found a significant reduction in infarct size and functional improvement after applying a different IPostC protocol. This could have resulted from a difference in the applied IPostC protocol (3 vs 6 episodes of reocclusion), differences in anesthetics (urethane/alfa-chloralose for the short reperfusion group and pentobarbital/ketamine for the survival experiments vs pentobarbital alone), and differences in the studied populations (mixed male and female vs male alone). Pentobarbital has been shown to have severe negative inotropic properties, and the cardioprotective effects of IPostC using pentobarbital anesthesia critically depend on the duration of index ischemia.[29] Finally, endogenous opioid peptides and their receptors play an important role in this adaptive phenomenon in the heart in a dose-dependent manner,[30] and, importantly, the choice of anesthetic combination might determine the postischemic Ca^{2+} leak and intracellular overload.[31]

Although some studies have shown a loss of cardioprotection in mouse models of diabetes mellitus,[2,22] we are the first to describe the functional and histologic benefits of IPostC in diabetic mice and an experimental model of the metabolic syndrome. We found a distinct contractility pattern with possible compensatory changes after IPostC in C57BL/6J mice. Moreover, we found a significant survival benefit in an experimental model of the metabolic syndrome after IPostC owing to a smaller infarct size and improved LV function. Therefore, our findings might result in new interest in a very powerful endogenous protective strategy and could open a new window of applying IPostC to a high-risk surgical population.

Study Limitations

Using mouse models as a preclinical model of myocardial infarction is challenging. They offer the opportunity to study different knockout models but demand very precise and accurate microsurgical handling. Although the results from mice experiments cannot be straightforwardly translated to the clinic, it offers a controlled environment to study disease aspects and treatment options. In humans, it is difficult to separate whether insulin resistance precedes or is secondary to the development of obesity. However, in the mouse models, diabetes appears to develop as a consequence of a failure to adequately increase the B-cell mass in response to obesity-induced insulin resistance.[32,33] Thus, mouse models of diabetes mellitus do not demonstrate the similarities for islet pathologic features observed in humans with type 2 diabetes mellitus. The ObOb and DKO model is based on leptin deficiency and creates an artificial environment in which the leptin levels are low, although in the patients with diabetes mellitus, the leptin levels tend to be greater. It is currently unknown to what extent leptin influences the IPostC protection directly.

CONCLUSIONS

IPostC is a powerful strategy to reduce the infarct size and LV impairment in C57BL6/J mice. Protection against lethal reperfusion injury remains; however, it might be reduced in obese diabetic (ObOb) mice and an experimental model of the metabolic syndrome (DKO mice). The cardioprotective effect of IPostC was sustained after 10 weeks and protected against adverse LV remodeling, with a specific contractility pattern revealed by myocardial tagging. Mortality was decreased after ischemia–reperfusion in the DKO mice owing to a reduction in infarct size and improved cardiac function. This cardioprotective technique might offer new opportunities for myocardial protection, even in a high-risk surgical population.

References

1. Zhao ZQ, Corvera JS, Halkos ME, Kerendi F, Wang NP, Guyton RA, et al. Inhibition of myocardial injury by ischemic postconditioning during reperfusion: comparison with ischemic preconditioning. *Am J Physiol Heart Circ Physiol*. 2003;285:579-88.
2. Bouhidel O, Pons S, Souktani R, Zini R, Berdeaux A, Ghaleh B. Myocardial ischemic postconditioning against ischemia-reperfusion is impaired in ob/ob mice. *Am J Physiol Heart Circ Physiol*. 2008;295:1580-6.
3. Tsang A, Hausenloy DJ, Mocanu MM, Yellon DM. Postconditioning: a form of "modified reperfusion" protects the myocardium by activating the phosphatidylinositol 3-kinase-Akt pathway. *Circ Res*. 2004;95:230-2.
4. Kin H, Zhao ZQ, Sun HY, Wang N-P, Corvera JS, Halkos ME, et al. Postconditioning attenuates myocardial ischemia–reperfusion injury by inhibiting events in the early minutes of reperfusion. *Cardiovasc Res*. 2004;62:74-85.
5. Argaud L, Gateau-Roesch O, Raisky O, Loufouat J, Robert D, Ovize M. Postconditioning inhibits mitochondrial permeability transition. *Circulation*. 2005;111:194-7.
6. Darling CE, Jiang R, Maynard M, Whittaker P, Vinten-Johansen J, Przyklenk K. Postconditioning via stuttering reperfusion limits myocardial infarct size in rabbit hearts: role of ERK1/2. *Am J Physiol Heart Circ Physiol*. 2005;289:1618-26.
7. Iliodromitis EK, Georgiadis M, Cohen MV, Downey JM, Bofilis E, Kremastinos DT. Protection from postconditioning depends on the number of short ischemic insults in anesthetized pigs. *Basic Res Cardiol*. 2006;101:502-7.
8. Staat P, Rioufol G, Piot C, Cottin Y, Cung TT, L'Huillier I, et al. Postconditioning the human heart. *Circulation*. 2005;112:2143-8.

PM

9. Thibault H, Piot C, Ovize M. Postconditioning in man. *Heart Fail Rev.* 2007;12: 245-8.

10. Laskey WK, Yoon S, Calzada N, Ricciardi MJ. Concordant improvements in coronary flow reserve and ST-segment resolution during percutaneous coronary intervention for acute myocardial infarction: a benefit of postconditioning. *Catheter Cardiovasc Interv.* 2008;72:212-20.

11. Thibault H, Piot C, Staat P, Bontemps L, Sportouch C, Rioufol G, et al. Long-term benefit of postconditioning. *Circulation.* 2008;117:1037-44.

12. Rosengren A, Welin L, Tsipogianni A, Wilhelmsen L. Impact of cardiovascular risk-factors on coronary heart-disease and mortality among middle-aged diabetic men—a general population study. *BMJ.* 1989;299:1127-31.

13. Hausenloy DJ, Boston-Griffiths E, Yellon DM. Cardioprotection during cardiac surgery. *Cardiovasc Res.* 2012;94:253-65.

14. Gateau-Roesch O, Argaud L, Ovize M. Mitochondrial permeability transition pore and postconditioning. *Cardiovasc Res.* 2006;70:264-73.

15. Bopassa JC, Ferrera R, Gateau-Roesch O, Couture-Lepetit E, Ovize M. PI 3-kinase regulates the mitochondrial transition pore in controlled reperfusion and postconditioning. *Cardiovasc Res.* 2006;69:178-85.

16. Gomez L, Paillard M, Thibault H, Derumeaux G, Ovize M. Inhibition of GSK3beta by postconditioning is required to prevent opening of the mitochondrial permeability transition pore during reperfusion. *Circulation.* 2008;117:2761-8.

17. Mykytenko J, Reeves JG, Kin H, Wang N-P, Zatta AJ, Jiang R, et al. Persistent beneficial effect of postconditioning against infarct size: role of mitochondrial K (ATP) channels during reperfusion. *Basic Res Cardiol.* 2008;103:472-84.

18. Boengler K, Schulz R, Heusch G. Loss of cardioprotection with ageing. *Cardiovasc Res.* 2009;83:247-61.

19. Van Der Mieren G, Flameng W, Herijgers P. The effect of type II diabetes and the metabolic syndrome on cardiac second window preconditioning. *Verh K Acad Geneeskd Belg.* 2008;70:221-44.

20. Mertens A, Verhamme P, Bielicki JK, Phillips MC, Quarck R, Verreth W, et al. Increased low-density lipoprotein oxidation and impaired high-density lipoprotein antioxidant defense are associated with increased macrophage homing and atherosclerosis in dyslipidemic obese mice—LCAT gene transfer decreases atherosclerosis. *Circulation.* 2003;107:1640-6.

21. Herbots L, Maes F, D'Hooge J, Claus P, Dymarkowski S, Mertens P, et al. Quantifying myocardial deformation throughout the cardiac cycle: a comparison of ultrasound strain rate, grey-scale m-mode and magnetic resonance imaging. *Ultrasound Med Biol.* 2004;30:591-8.

22. Przyklenk K, Maynard M, Greiner DL, Whittaker P. Cardioprotection with postconditioning: loss of efficacy in murine models of type-2 and type-1 diabetes. *Antioxid Redox Signal.* 2011;14:781-90.

23. Wagner C, Kloeting I, Strasser RH, Weinbrenner C. Cardioprotection by postconditioning is lost in WOKW rats with metabolic syndrome: robe of glycogen synthase kinase 3P. *J Cardiovasc Pharmacol.* 2008;52:430-7.

24. Ferdinandy P, Schulz R, Baxter GF. Interaction of cardiovascular risk factors with myocardial ischemia/reperfusion injury, preconditioning, and postconditioning. *Pharmacol Rev.* 2007;59:418-58.

25. Freixa X, Bellera N, Ortiz-Perez JT, Jiménez M, Paré C, Bosch X, et al. Ischaemic postconditioning revisited: lack of effects on infarct size following primary percutaneous coronary intervention. *Eur Heart J.* 2012;33:103-12.

26. Abd-Elfattah AS, Aly H, Hanan S, Wechsler AS. Myocardial protection in beating heart cardiac surgery: I: pre- or postconditioning with inhibition of es-ENT1 nucleoside transporter and adenosine deaminase attenuates post-MI reperfusion-mediated ventricular fibrillation and regional contractile dysfunction. *J Thorac Cardiovasc Surg.* 2012;144:250-5.

27. Luo WJ, Li B, Lin GQ, Huang RM. Postconditioning in cardiac surgery for tetralogy of Fallot. *J Thorac Cardiovasc Surg.* 2007;133:1373-4.

28. Mentzer RM. Myocardial protection in heart surgery. *J Cardiovasc Pharmacol Ther.* 2011;16:290-7.

29. Manintveld OC, te Lintel Hekkert M, van den Bos EJ, Suurenbroek GM, Dekkers DH, Verdouw PD, et al. Cardiac effects of postconditioning depend critically on the duration of index ischemia. *Am J Physiol Heart Circ Physiol.* 2007; 292:1551-60.

30. Karlsson LO, Bergh N, Li L, Bissessar E, Bobrova I, Gross GJ, et al. Dose-dependent cardioprotection of enkephalin analogue Eribis peptide 94 and cardiac expression of opioid receptors in a porcine model of ischaemia and reperfusion. *Eur J Pharmacol.* 2012;674:378-83.

31. Zaugg M, Wang L, Zhang L, Lou PH, Lucchinetti E, Clanachan AS. Choice of anesthetic combination determines Ca2+ leak after ischemia-reperfusion injury in the working rat heart: favorable versus adverse combinations. *Anesthesiology.* 2012;116:648-57.

32. Baetens D, Stefan Y, Ravazzola M, Malaisselagae F, Coleman DL, Orci L. Alteration of islet cell-populations in spontaneously diabetic mice. *Diabetes.* 1978;27: 1-7.

33. Cefalu WT. Animal models of type 2 diabetes: clinical presentation and pathophysiological relevance to the human condition. *Ilar J.* 2006;47:186-98.

PM